

A Mass Spectrometric Study of the $\text{NH}_2 + \text{NO}_2$ Reaction

J. Park and M. C. Lin*

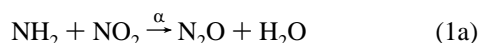
Department of Chemistry, Emory University, Atlanta, Georgia 30322

Received: November 7, 1996; In Final Form: February 4, 1997[⊗]

The total rate constant and product branching ratios of the $\text{NH}_2 + \text{NO}_2$ reaction have been determined in the temperature range of 300–910 K using a pulsed laser photolysis/mass spectrometric technique by probing H_2O and N_2O product formation and NO_2 reactant decay. A weighted least-squares fit of our result for the total rate constant yields the following expression: $k_1 = (8.1 \pm 0.33) \times 10^{16} T^{-1.44} \exp(-135/T) \text{ cm}^3/(\text{mol}\cdot\text{s})$. The product branching ratio for the $\text{N}_2\text{O} + \text{H}_2\text{O}$ channel of the $\text{NH}_2 + \text{NO}_2$ reaction obtained by modeling the absolute N_2O product yield near or at its plateau value gives 0.19 ± 0.02 without significant temperature dependence, confirming our earlier result obtained by using a high-gain amplifier with no time-resolved information (ref 18).

I. Introduction

The reaction of NH_2 with NO_2 has been considered to be one of the most important steps in the removal of NO_2 by NH_3 ^{1–4} and in the decomposition of ammonium nitrate (AN) and ammonium dinitramide (ADN)^{5–7} because of its high probability of producing atomic and radical chain carriers. The possible major product channels are^{8–11}



The H_2NO formed in reaction 1b can generate one of the most reactive and efficient radicals in the deNO_x and propellant combustion processes, H, by the sequential decomposition reactions: $\text{H}_2\text{NO} + \text{M} = \text{H} + \text{HNO} + \text{M}$ and $\text{HNO} + \text{M} = \text{H} + \text{NO} + \text{M}$. Accordingly, the kinetics and the product branching ratios of the $\text{NH}_2 + \text{NO}_2$ reaction are important for the quantitative understanding of the NH_3 deNO_x and the decomposition and/or combustion of AN, ADN, and NH_3 .

Although the total rate constant of the $\text{NH}_2 + \text{NO}_2$ reaction has been measured by many groups,^{12–17} the existing experimental data, which exhibit a large negative temperature dependence, have a significant spread in their absolute values throughout the temperature range studied. In a recent report,¹⁸ we described the noticeable effect of the discrepancy on kinetically modeled product branching ratios. Accordingly, it is necessary to measure the total rate constant reliably in order to resolve the discrepancy and to provide accurate product branching ratios for practical applications. In this paper, we present the results of the total rate constant and *additional* product branching ratio data obtained from a new series of experiments using a pulsed laser photolysis/mass spectrometric technique with a newly acquired fast amplifier.

II. Experiment

The total rate constant and the product branching ratio measurements for the $\text{NH}_2 + \text{NO}_2$ reaction were performed in the temperature range of 300–910 K by pulsed laser photolysis/mass spectrometry employing the high-pressure sampling technique developed by Saalfeld,¹⁹ Gutman,²⁰ and co-workers.

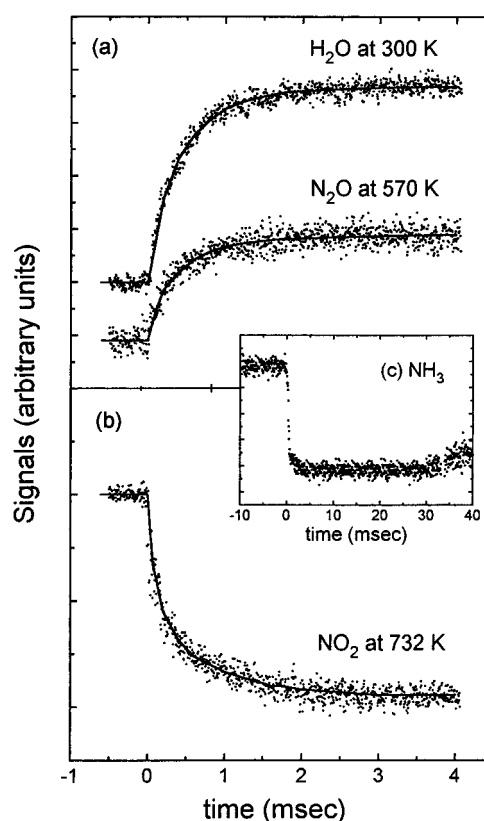


Figure 1. Time-resolved reactant and product signals. Conditions are given in Table 1.

A detailed description of the apparatus can be found elsewhere,²¹ and only a brief one is given here.

The experiment was carried out in a quartz tubular Saalfeld-type reaction tube (which has an inner diameter of 10 mm and a length of 140 mm) with a 120 μm conical sampling hole mounted perpendicular to a quadrupole mass spectrometer (QMS, Extrel Model C50). The NH_2 radical was generated by the photodissociation of NH_3 at 193 nm with an ArF excimer laser, typically with 1–8% NH_3 conversion depending on the reaction temperature and photolysis laser energy employed.

All experimental runs were performed under slow-flow conditions using different compositions of $\text{NH}_3/\text{NO}_2/\text{He}$ at a constant total pressure, varied from 1.3 to 8.3 Torr. The reactants and the helium buffer gas were premixed in a stain-

* Corresponding author; e-mail: chemmcl@emory.edu.

[⊗] Abstract published in *Advance ACS Abstracts*, March 15, 1997.

TABLE 1: Summary of the Total Rate Constant Data for the $\text{NH}_2 + \text{NO}_2$ Reaction^a

<i>T</i> (K)	<i>P</i>	$[\text{NH}_3]_0$	$[\text{NO}_2]_0$	$[\text{NH}_2]_0$	$[\text{O}]_0$	$k_1 \times 10^{12} \text{ cm}^3/(\text{mol}\cdot\text{s})^b$
300	5090–5320	74.71–77.84	22.33–42.70	7.39–7.70	0.21–0.23	13.9 ± 0.68
300	1820–2120	27.63–27.83	7.986–23.07	2.75–2.73	0.08–0.23	13.8 ± 0.46^c
310	4160–4450	84.88–93.86	31.88–82.04	7.38–8.16	0.17–0.44	12.2 ± 0.66
337	5150–5380	76.39–80.07	22.56–43.13	6.49–6.64	0.27–0.96	12.4 ± 0.73
373	4270–4540	74.82–98.50	31.16–65.04	6.59–6.85	0.25–0.50	10.6 ± 1.68
380	5150–5380	76.56–79.81	22.65–43.06	6.48–6.75	0.18–0.34	11.5 ± 0.56
403	5730–6200	130.5–145.1	27.03–76.27	5.86–6.52	0.24–0.67	10.7 ± 0.84
452	5200–5460	77.87–80.76	22.62–43.59	6.40–6.64	0.43–0.46	10.4 ± 0.73
496	6270–6450	135.7–160.4	26.57–79.08	6.10–7.20	0.32–0.96	7.93 ± 0.61
503	5980–6230	106.6–113.2	22.97–62.27	8.77–9.84	0.28–0.77	7.45 ± 1.55
570	5800–6300	106.6–114.5	22.50–62.85	5.25–5.60	0.33–0.93	6.28 ± 0.36
653	4640–5220	103.1–108.5	35.40–95.75	4.86–5.11	0.64–1.72	5.72 ± 0.27
732	4680–5200	103.8–110.6	35.60–94.10	3.76–4.01	0.74–1.96	4.72 ± 0.55
810	7020–7980	161.9–168.8	53.30–145.6	3.14–3.27	1.27–3.46	3.85 ± 0.26
910	7340–8270	178.6–187.5	49.40–143.6	2.17–2.28	1.36–3.95	4.32 ± 0.54

^a The units of total pressure and all concentrations are in mTorr. ^b Average values from 4–5 experimental runs based on the decay time of NO_2 and the rise times of N_2O and H_2O ; the uncertainty represents 1σ . ^c Total rate constant was measured with a reactor coated with concentrated H_3PO_4 .

less steel bellows tube before introduction into the reactor. For the experiment at elevated temperatures, the reactor was heated with nichrome ribbon insulated with ceramic wool. The reactor temperature could be varied from room temperature up to 1200 K.

The positive ion signals of NH_3 , H_2O , N_2O , NO_2 , and O_2 were generated by electron impact ionization at 70 eV and detected with QMS mass selection. Time-resolved transient signals were averaged over 100–200 laser shots with 1 Hz repetition rate and stored in a Nicolet 450 Digital Waveform Acquisition System for later analysis.

NH_3 (Aldrich), N_2O (Matheson), and H_2O (deionized) were purified by standard trap-to-trap distillation using appropriate slush baths. NO_2 (Matheson) was purified by adding an excess quantity of O_2 overnight (to convert any NO impurity into NO_2); the unreacted O_2 was removed by trap-to-trap distillation. O_2 (99.9995%) and He (99.9995%) were used without further purification.

III. Results

1. Total Rate Constant Measurement. The time-resolved concentration profiles of the formation of the H_2O and N_2O products and the decay of the NO_2 reactant were directly measured for the determination of the total rate constant of the $\text{NH}_2 + \text{NO}_2$ reaction using various mixtures of $\text{NH}_3/\text{NO}_2/\text{He}$ with a total pressure of 1.8–8.3 Torr. By changing the composition of NH_3/NO_2 and/or the power of the photolysis laser, the $[\text{NO}_2]/[\text{NH}_2]$ reactant ratio could be varied from 2.3 to 44.5 in the temperature range of 300–910 K. Figure 1 shows typical time-resolved transient signals of H_2O , N_2O , and NO_2 . These signals were taken with different reaction conditions and were averaged with 100–200 laser pulses at 1 Hz repetition rate. As shown in the inset of the figure, the NH_3 signal dropped immediately after the photodissociation pulse and remained constant for about 30–40 ms until a fresh sample filled the reactor. Kinetic and branching ratio measurements were carried out within the 30–40 ms period. The measured ion signals for each species were directly converted to absolute concentrations with standard calibration mixtures under exactly the same *P*, *T* conditions as employed in the experimental runs.

The experimental conditions and results of the total rate constant measurement are summarized in Table 1. For the total rate constant, the initial rates of NO_2 decay as well as N_2O and H_2O formation were kinetically modeled with the SENKIN program²² using a set of reactions summarized in Table 2 to simulate the early kinetics of the laser-initiated $\text{NH}_3/\text{NO}_2/\text{He}$

system at each temperature. The modeled values from the three independent sets of data (i.e., NO_2 , N_2O , and H_2O) agree within the typical scatter ($\pm 10\%$) shown in Table 1. In order to take into account competing secondary reactions, kinetic modeling is essential and often mandatory even under a pseudo-first-order condition (i.e., $[\text{NO}_2] \gg [\text{NH}_2]$). In our kinetic modeling, we also included the initial O (^3P) concentration produced by the photodissociation of NO_2 .¹⁸ The amount of O atoms was measured by the depletion of NO_2 and the formation of O_2 in the absence of NH_3 at each temperature. The time-resolved concentration profiles could be quantitatively fitted to the kinetically modeled values as illustrated in Figure 1 by solid curves.

The modeled total rate constants summarized in Table 1 were fitted to the standard three-parameter equation, $k_1 = AT^B \exp(-C/T)$, by a weighted least-squares method²⁴ which yielded the following expression for the temperature range of 300–910 K:

$$k_1 = (8.1 \pm 0.33) \times 10^{16} T^{-1.44} \exp(-135/T) \text{ cm}^3/(\text{mol}\cdot\text{s})$$

2. Product Branching Ratio Determination. Product channel branching ratios for the $\text{NH}_2 + \text{NO}_2$ reaction were determined by the plateau or near-plateau values of N_2O signals using various mixtures of $\text{NH}_3/\text{NO}_2/\text{He}$. As in our previous product branching ratio determination for $\text{NH}_2 + \text{NO}$,^{21,23} all of our earlier measurements for $\text{NH}_2 + \text{NO}_2$ product branching were made with a high-gain amplifier for the plateau (typically 5–10 ms) concentration determination without the rising kinetic information. The advantage of such measurements is their stronger signals and thereby a shorter data acquisition time.

In the present study, the N_2O yields in or near the plateau region were kinetically modeled to obtain α_1 [$\alpha_1 = k_{1a}/(k_{1a} + k_{1b})$], the branching ratio for $\text{NH}_2 + \text{NO}_2 \rightarrow \text{N}_2\text{O} + \text{H}_2\text{O}$ (1a), by keeping the total rate constant ($k_1 = k_{1a} + k_{1b}$) determined from the rise times of the signals unchanged while varying the relative values of k_{1a} and k_{1b} . As in the determination for the total rate constant, kinetic modeling of the branching ratio was performed for each experimental run using the reaction mechanism given in Table 2 in order to account for the effect of secondary reactions. The experimental conditions, product yields with kinetically modeled results, and branching ratios are summarized in Table 3. The resulting branching ratios are presented in Figure 3 and compared with previously reported values,^{2,25} including our earlier results obtained by the high-gain amplifier.¹⁸ As shown in the figure, the branching ratio of the $\text{N}_2\text{O} + \text{H}_2\text{O}$ product channel, determined by fitting the

TABLE 2: Reactions and Rate Constants^a Used in the Kinetic Modeling of the NH₂ + NO₂ System^b

reaction	A	n	E _a
1a. NH ₂ + NO ₂ = N ₂ O + H ₂ O	1.54E+16	-1.44	268 ^c
1b. NH ₂ + NO ₂ = H ₂ NO + NO	6.56E+16	-1.44	268 ^c
2. OH + NH ₃ = H ₂ O + NH ₂	2.00E+12	0.00	1830
3. NH + H = N + H ₂	3.00E+13	0.00	0
4. NH + N = N ₂ + H	3.00E+13	0.00	0
5. NH + NH = N ₂ + H ₂	2.50E+13	0.00	0
6. NH + NO = N ₂ + OH	2.90E+13	-0.23	0
7. NH + NO = N ₂ O + H	2.20E+14	-0.40	0
8. NH + OH = HNO + H	2.00E+13	0.00	0
9. NH + OH = N + H ₂ O	5.00E+11	0.50	2000
10. NH + HONO = NH ₂ + NO ₂	1.00E+13	0.00	0
11. NH ₂ + H = NH + H ₂	4.00E+13	0.00	3656
12. NH ₂ + HNO = NH ₃ + NO	3.60E+07	1.60	-1252
13. NH ₂ + HONO = NH ₃ + NO ₂	7.11E+01	3.00	4942
14. NH ₂ + NH = N ₂ H ₂ + H	1.50E+15	-0.50	0
15. NH ₂ + NH ₂ = NH + NH ₃	5.00E+13	0.00	9995
16. NH ₂ + NH ₂ = N ₂ H ₂ + H ₂	5.00E+11	0.00	0
17. NH ₂ + NO = N ₂ H + OH	8.40E+09	0.53	-998
	9.19E+22	-3.02	9589
18. NH ₂ + NO = N ₂ + H ₂ O	8.28E+14	-0.93	-382
	3.40E+14	-0.98	-2605
19. NH ₂ + OH + M = H ₂ NOH + M	5.70E+24	-3.00	0
20. NH ₂ + OH = NH + H ₂ O	4.00E+06	2.00	1000
21. NH ₃ + M = NH ₂ + H + M	2.20E+16	0.00	93468
22. NH ₃ + H = H ₂ + NH ₂	6.36E+05	2.39	10171
23. N ₂ H + H = H ₂ + N ₂	1.00E+14	0.00	0
24. N ₂ H + M = H + N ₂ + M	1.00E+14	0.00	3000
25. N ₂ H + OH = H ₂ O + N ₂	5.00E+13	0.00	0
26. N ₂ H + NH = NH ₂ + N ₂	5.00E+13	0.00	0
27. N ₂ H + NO = HNO + N ₂	5.00E+13	0.00	0
28. N ₂ H ₂ + H = N ₂ H + H ₂	5.00E+13	0.00	1000
29. N ₂ H ₂ + O = NH ₂ + NO	1.00E+13	0.00	1000
30. N ₂ H ₂ + O = N ₂ H + OH	2.00E+13	0.00	1000
31. N ₂ H ₂ + OH = N ₂ H + H ₂ O	1.00E+13	0.00	1000
32. N ₂ H ₂ + NO = NH ₂ + N ₂ O	3.00E+12	0.00	0
33. N ₂ H ₂ + NH = N ₂ H + NH ₂	1.00E+13	0.00	1000
34. N ₂ H ₂ + NH ₂ = N ₂ H + NH ₃	1.00E+13	0.00	1000
35. O + NO ₂ = O ₂ + NO	1.00E+13	0.00	600
36. OH + H ₂ = H ₂ O + H	1.20E+09	0.00	0
37. OH + HNO = H ₂ O + NO	3.60E+13	0.00	0
38. OH + HONO = H ₂ O + NO ₂	4.00E+12	0.00	0
39. OH + NO + M = HONO + M	1.00E+28	-2.51	-68
40. OH + OH = H ₂ O + O	6.00E+08	1.30	0
41. OH + OH + M = H ₂ O ₂ + M	5.70E+24	-3.00	0
42. H + H + M = H ₂ + M	1.00E+18	-1.00	0
43. H + HNO = H ₂ + NO	4.50E+11	0.70	650
44. H + NO + M = HNO + M	5.40E+15	0.00	-600
45. H + NO ₂ = OH + NO	3.50E+14	0.00	1500
46. H + OH + M = H ₂ O + M	1.60E+22	-2.00	0
47. HNO + O = NO + OH	1.00E+13	0.00	0
48. HNO + NO = N ₂ O + OH	2.00E+12	0.00	26000
49. HNO + NO ₂ = HONO + NO	6.00E+11	0.00	2000
50. HNO + HNO = N ₂ O + H ₂ O	4.00E+12	0.00	5000
51. HONO + H = NO ₂ + H ₂	1.20E+12	0.00	7350
52. HONO + O = NO ₂ + OH	1.20E+13	0.00	6000
53. HONO + HONO = NO + NO ₂ + H ₂ O	2.30E+12	0.00	8400
54. H ₂ NO + M = HNO + H + M	5.00E+16	0.00	50000
55. H ₂ NO + NO = HNO + HNO	2.00E+07	2.00	13000
56. H ₂ NO + NO ₂ = HNO + HONO	6.00E+11	0.00	2000
57. H ₂ NO + NH ₂ = HNO + NH ₃	3.00E+12	0.00	1000
58. HNNO + NO = N ₂ + HONO	2.60E+11	0.00	1620
59. HNNO + NO = N ₂ H + NO ₂	3.20E+12	0.00	540
60. NO ₂ + M = NO + O + M	1.10E+16	0.00	66000
61. N ₂ O + M = N ₂ + O + M	4.40E+14	0.00	56100

^a Rate constants are defined by $k = AT^n \exp(-E_a/RT)$ and in units cm³, mol, and s; E_a is in the unit of cal/mol. $E + n \equiv \times 10^n$. ^b Reference 21. ^c This work.

absolute number density of N₂O to modeled yield, was found to be 0.19 ± 0.02 without significant temperature dependence. In Table 3, the calculated of H₂O yields are compared with the measured values.

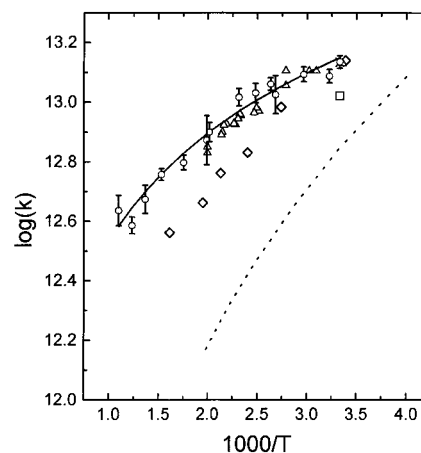
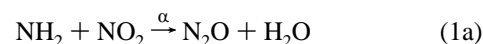


Figure 2. Arrhenius plot for the total rate constant of the NH₂ + NO₂ reaction: (○ and solid line) this work; (dashed line) ref 12; (×) ref 15; (□) ref 17; (◇), ref 16; (△) ref 13.

IV. Discussion

1. Reaction Mechanism. The mechanism of the NH₂ + NO₂ reaction has been investigated in detail by Mebel et al.¹¹ through a high-level ab initio calculation. The result indicates that the reaction takes place primarily by the following two channels:



Other possible channels leading to the formation of N₂ + H₂O₂, N₂ + 2OH and HN₂O + OH require high reaction barriers which are inconsistent with the observed negative activation energy.

Reaction 1a occurs by the initial formation of the vibrationally excited H₂NNO₂ intermediate which rapidly isomerizes to HNN-(OH)O, prior to the elimination of H₂O, giving the N₂O product. The transition states for the isomerization and H₂O elimination lie several kcal/mol below the NH₂ + NO₂ reactants and thus no apparent positive activation energy is required for N₂O production.

Reaction 1b is expected to take place via the vibrationally excited H₂NNONO intermediate which fragments directly to yield the H₂NO + NO products. Both the association and decomposition transition states, as in the isoelectronic CH₃ + NO₂ → CH₃ONO → CH₃O + NO reaction, are poorly defined and, accordingly, have not yet been characterized by our ab initio calculation.¹¹ Rate constant calculations for both product channels require a variational statistical approach using well-mapped potential energy surfaces.²⁶

2. Total Rate Constant. The total rate constants presented in Table 1 and Figure 2 exhibit a strong negative temperature dependence which is consistent with the results of other studies summarized in the figure. Our result, given by open circles in Figure 2, merges closely with that of Kurasawa and Lesclaux.¹³ However, it deviates noticeably from those of Bulatov et al.,¹⁶ Pagsberg et al.,¹⁷ and Wagner and co-workers,¹² particularly the latter which is lower than ours by a factor of 2 at room temperature and by more than a factor of 5 at 500 K. The origin of such an unusually large deviation is perplexing. It is worth noting that the rate constants given for other NH₂ reactions (i.e., with NO, C₂H₂, and C₂H₄) in the same paper were also found to be significantly lower than those reported by related studies.²⁷

In order to test the possible effect of the reactor surface, we have also measured the total rate constant at room temperature using a reactor treated with concentrated H₃PO₄. After pro-

TABLE 3: Typical Reaction Conditions, Product Yields, and Kinetically Modeled Values of α at the Temperatures Studied^a

temp (K)	P_{tot}	[NH ₃] ₀	[NO ₂] ₀	[NH ₂] ₀	[O] ₀	α	[N ₂ O] _f ^b		[H ₂ O] _f ^b	
							exp	calc	exp	calc
300 ^c	4200	56.20	43.76	2.37	0.47	0.18	0.64	0.62	3.35	2.81
300	4480	65.37	53.84	2.76	1.37	0.18	0.72	0.68	4.13	2.92
310	1280	16.69	15.44	1.33	1.42	0.20	0.33	0.34	1.50	1.45
403	6200	140.9	56.25	6.64	0.99	0.20	1.71	1.73	12.2	11.1
428 ^c	5180	65.73	50.82	2.18	6.20	0.20	0.71	0.76	3.68	2.89
496	6270	143.2	56.51	5.97	1.39	0.20	1.31	1.68	9.14	8.53
520 ^c	1570	24.27	21.33	1.32	0.35	0.18	0.34	0.36	1.84	1.71
585	5400	69.11	51.78	1.68	1.84	0.20	0.58	0.61	3.17	2.52
600	5310	137.9	46.86	4.26	1.52	0.18	1.24	1.20	7.21	5.52
640 ^c	5200	64.58	46.41	1.40	2.46	0.20	0.44	0.43	2.95	2.16
732	5200	103.5	93.10	3.98	3.97	0.18	1.13	1.20	5.71	5.51
800 ^c	5400	70.29	51.10	1.09	3.48	0.20	0.38	0.37	2.55	1.88
824	1800	18.06	14.00	0.44	0.73	0.20	0.26	0.26	1.29	1.26
903 ^c	5400	69.53	50.33	1.24	3.28	0.20	0.42	0.45	3.48	2.41
910	8270	177.0	139.5	3.61	7.90	0.18	1.17	1.19	6.43	5.36
990 ^c	6400	98.80	75.31	1.87	4.62	0.18	0.63	0.63	3.22	2.83

^a The units of pressures and concentrations are in mTorr. ^b The signal amplitude was taken $t = 3.6$ ms. ^c Reported in ref 18.

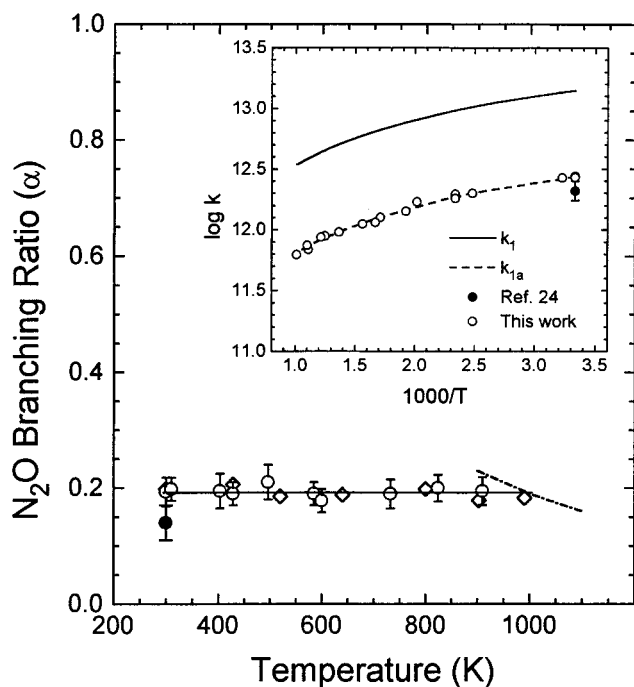


Figure 3. Branching ratio of $\text{NH}_2 + \text{NO}_2 \rightarrow \text{N}_2\text{O} + \text{H}_2\text{O}$ (α) as a function of temperature: (○) this work; (◇) ref 18; (●) ref 24; (dash-dotted line) ref 2. Inset: Arrhenius plots for k_1 and k_{1a} (α).

longed annealing at 1000 K, the treated reactor provided essentially the same result for k_1 at the lowest pressure studied as the untreated quartz reactor did (see Table 1). A similar test for $\text{NH}_2 + \text{NO}_2$ ²¹ and $\text{CH}_3 + \text{CH}_3$ ²⁸ reactions at 2 Torr pressure did not reveal detectable surface effects either.

3. Product Branching Ratios. The branching ratio for the production of N_2O has been reported in our recent communication¹⁸ for the same temperature range (300–990 K), based entirely on the results of our mass spectrometric measurement with the high-gain signal amplifier, assuming the total rate constant $k_1 = 1.08 \times 10^{12} T^{0.11} \exp(+597/T) \text{ cm}^3/(\text{mol}\cdot\text{s})$.² These results (with a minor adjustment in the high-temperature region because of the small difference in the k_1 used for modeling) are also summarized in Table 3 and compared with the present data in Figure 3. The new and old data agree closely, and together they give a temperature-independent branching ratio for N_2O production, $\alpha = 0.19 \pm 0.02$. Combining this value with the total rate constant expression above gives rise to the absolute rate constant expression:

$$k_{1a} = 1.54 \times 10^{16} T^{-1.44} \exp(-135/T) \text{ cm}^3/(\text{mol}\cdot\text{s})$$

In Figure 3, we also compare our branching ratio data with that of Quandt and Hershberger,²⁴ 0.14 ± 0.03 , measured at room temperature by infrared diode laser absorption spectrometry, and with the modeled value of Glarborg et al.² from their study of the thermal reaction of NH_3 with NO_2 at 850–1350 K. Altogether, these recent results suggest convincingly that α and β are insensitive to temperature change between 300 and 1350 K. This, in turn, suggests that k_{1a} and k_{1b} have a similar temperature dependence as k_1 over the same temperature range.

After the submission of the present work, the $\text{NH}_2 + \text{NO}_2$ product branching data determined at room temperature by Pagsberg and co-workers²⁹ came to our attention. By pulsed radiolysis with time-resolved infrared diode laser absorption spectrometry, they measured the concentrations of N_2O and NO as well as the total decay rates of NH_2 . Although their total rate constant, $k_1 = 8.1 \times 10^{12} \text{ cm}^3/(\text{mol}\cdot\text{s})$, agrees with the value reported earlier by that group¹⁷ (see Figure 2) at room temperature, it is noticeably lower than the majority of existing data, including the present work. However, their value of α , 0.59 ± 0.03 , is 3 times higher than ours and is inconsistent with the values of Quandt and Hershberger²⁵ as well as Glarborg et al.² This large discrepancy is unsupported by the most recent remeasured value of Hershberger, $\alpha = 0.25$ at room temperature.³⁰

4. Sensitivity Analysis. Our values of α were determined primarily by kinetic modeling of the limiting yields of N_2O . Although H_2O is a coproduct of reaction 1a, it was not utilized for the evaluation of α because of the expected large contribution from many secondary reactions such as $\text{OH} + \text{NH}_3 \rightarrow \text{H}_2\text{O} + \text{NH}_2$. This is clearly illustrated by the result of our sensitivity analysis with SENKIN²² presented in Figure 4.

As shown in the figure, the predominant process contributing to the formation of N_2O is reaction 1a, with (1b) playing a strong opposing role. This makes N_2O the best product for the determination of α because of the added sensitivity—a small adjustment in the value of α by varying k_{1a} while keeping the sum $k_1 = k_{1a} + k_{1b}$ constant in the fitting process results in a large change in the calculated N_2O yield.

However, the yields of H_2O , as revealed by the result in Figure 4, indicate that the $\text{OH} + \text{NH}_3$ reaction (2) rather than (1b) is the dominating contributory process even at 640 K. The sources of the OH radical are numerous, for example, $\text{H} + \text{NO}_2$ and $\text{NH}_2 + \text{NO}$. The data summarized in the last entry for $[\text{H}_2\text{O}]_f$ in Table 3 also reflects this fact: the H_2O concentration

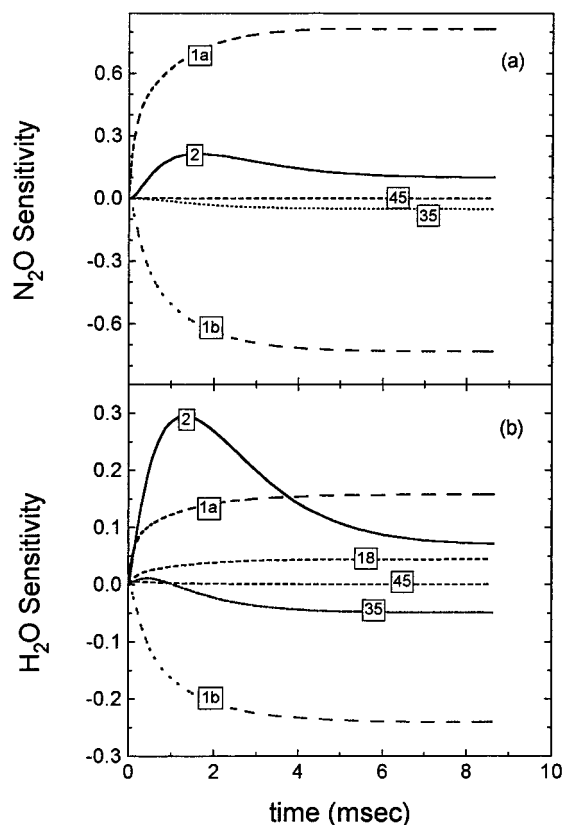


Figure 4. Sensitivity analyses for (a) N_2O and (b) H_2O at 640 K.

measured at $t = 3.6$ ms is typically 5–6 times greater than that of N_2O . Thus, H_2O is not an ideal product for the modeling of α . It is gratifying to note that the observed concentration of H_2O could be reasonably predicted with the mechanism used in the modeling.

V. Conclusions

The total rate constant and the product branching ratio of the $\text{NH}_2 + \text{NO}_2$ reaction have been determined over the temperature range of 300–990 K by a pulsed laser photolysis/mass spectrometric method. The kinetic modeling of the observed rates of N_2O formation and NO_2 decay allows us to determine the total rate constant of $\text{NH}_2 + \text{NO}_2$ between 300 and 910 K, $k_1 = (8.1 \pm 0.33) \times 10^{16} T^{-1.44} \exp(-135/T) \text{ cm}^3/(\text{mol} \cdot \text{s})$. From the limiting yields of N_2O measured in the plateau region of the concentration profiles, the branching ratio for the product channel $\text{NH}_2 + \text{NO}_2 \rightarrow \text{N}_2\text{O} + \text{H}_2\text{O}$ (1a) was determined to be 0.19 ± 0.02 , independent of temperature over the range studied. This result compares reasonably with recently reported values at room temperature as well as in the high-temperature regime (850–1350 K).

The product branching ratio and the total rate constant for the pivotal $\text{NH}_2 + \text{NO}_2$ process determined in this study make it possible for the combustion community to elucidate more reliably the complex chemistry of the NH_3 de NO_x and ammonium nitrate and ammonium dinitramide propellant combustion processes.

Acknowledgment. The authors gratefully acknowledge the support of this work by the Office of Naval Research (contract no. N00014-89-J-1949) under the direction of Dr. R. S. Miller.

References and Notes

- (1) Lyon, R. K. U.S. Patent 3, 900, 559, 1975.
- (2) Glarborg, P.; Dam-Johansen, K.; Miller, J. A. *Int. J. Chem. Kinet.* **1995**, *27*, 1207.
- (3) Rosser, W. A., Jr.; Wise, H. J. *Chem. Phys.* **1956**, *29*, 1078.
- (4) Bedford, G.; Thomas, J. H. *J. Chem. Soc., Faraday Trans. 1*, **1972**, *68*.
- (5) Brill, T. B.; Brush, P. J.; Patil, D. G. *Combust. Flame* **1993**, *92*, 7788.
- (6) Rossi, M. J.; Bottaro, J. C.; McMillen, D. F. *Int. J. Chem. Kinet.* **1993**, *25*, 549, 1993.
- (7) Mebel, A. M.; Lin, M. C.; Morokuma, K.; Melius, C. F. *J. Phys. Chem.* **1995**, *95*, 6842.
- (8) Saxon, R. P.; Yoshimine, M. *J. Phys. Chem.* **1989**, *93*, 3130.
- (9) Seminario, J. M.; Politzer, P. *Int. J. Quantum Chem. Symp.* **1992**, *26*, 497.
- (10) Melius, C. F. In *Chemistry and Physics of Energetic Materials*; Bulusu, S., Ed.; NATO ASI 309; 1990; p 21.
- (11) Mebel, A. M.; Hsu, C.-C.; Lin, M. C.; Morokuma, K. *J. Chem. Phys.* **1995**, *103*, 5640.
- (12) Hack, W.; Schake, H.; Schroter, H.; Wagner, H.-Gg. *Proceedings of the 7th International Symposium on Combustion*; The Combustion Institute; Pittsburgh, PA, 1979; p 505.
- (13) Kurasawa, H.; Lesclaux, R. *Chem. Phys. Lett.* **1979**, *66*, 602.
- (14) Whyte, A. R.; Phillips, L. F. *Chem. Phys. Lett.* **1983**, *102*, 451.
- (15) Xiang, T. X.; Torres, L. M.; Guillery, W. A. *J. Chem. Phys.* **1985**, *83*, 1623.
- (16) Bulatov, V. P.; Ioffe, A. A.; Lozovsky, V. A.; Sarkisov, O. M. *J. Chem. Phys.* **1985**, *82*, 1623.
- (17) Pagsberg, P.; Sztuba, B.; Ratajczak, E.; Sillesen, A. *Acta Chem. Scand.* **1991**, *45*, 329.
- (18) Park, J.; Lin, M. C. *Int. J. Chem. Kinet.* **1996**, *28*, 879.
- (19) Wyatt, J. R.; DeCorpo, J. J.; McDowell, W. V.; Saafeld, F. E. *Rev. Sci. Instrum.* **1974**, *45*, 916.
- (20) Slagle, I. R.; Gutman, D. *J. Am. Chem. Soc.* **1985**, *107*, 5342.
- (21) Park, J.; Lin, M. C. *J. Phys. Chem. A* **1997**, *101*, 5.
- (22) Lutz, A. E.; Lee, R. K.; Miller, J. A. SENKIN: A FORTRAN Program for Predicting Homogeneous Gas-Phase Chemical Kinetics with Sensitivity Analysis; Sandia National Laboratories Report No. SANDIA 89-8009, 1989.
- (23) Park, J.; Lin, M. C. *J. Phys. Chem.* **1996**, *100*, 3317.
- (24) Cvetanovic, R. J.; Singleton, D. L.; Paraskevopoulos, G. *J. Phys. Chem.* **1979**, *83*, 50.
- (25) Quandt, R.; Hershberger, J. *J. Phys. Chem.* **1996**, *100*, 9407.
- (26) Wardlaw, D. M.; Marcus, R. A. *Adv. Chem. Phys.* **1987**, *70*, 231.
- (27) Mallard, W. G.; Westley, F.; Herron, J. T.; Hampton, R. F. NIST Chemical Kinetics Database, 1994.
- (28) Park, J.; Lin, M. C. *J. Phys. Chem. A* **1997**, *101*, 14.
- (29) Meunier, H.; Pagsberg, P.; Sillesen, A. *Chem. Phys. Lett.* **1996**, *261*, 277.
- (30) Hershberger, J. F., private communication.